Journal of Protein Chemistry, Vol. 15, No. 4, 1996

Conformational Effects in the p53 Protein of Mutations Induced During Chemical Carcinogenesis: Molecular Dynamic and Immunologic Analyses

Paul W. Brandt-Rauf,[1,6] James M. Chen,[2] Marie-Jeanne Marion,[3] Steven J. Smith,[1] Jiin-Chyuan Luo,[1] Walter Carney,[4] and Matthew R. Pincus[5]

Received February 27, 1996

The tumor suppressor gene p53 has been identified as the most frequent target of genetic alterations in human cancers. Vinyl chloride, a known human carcinogen that induces the rare sentinel neoplasm angiosarcoma of the liver, has been associated with specific A→T transversions at the first base of codons 249 and 255 of the p53 gene. These mutations result in an Arg→Trp amino acid substitution at residue 249 and an Ile→Phe amino acid substitution at residue 255 in a highly conserved region in the DNA-binding core domain of the p53 protein. To determine the effects of these substitutions on the three-dimensional structure of the p53 protein, we have performed molecular dynamics calculations on this core domain of the wild-type and the Trp-249 and Phe-255 mutants to compute the average structures of each of the three forms. Comparisons of the computed average structures show that both mutants differ substantially from the wild-type structure in certain common, discrete regions. One of these regions (residues 204–217) contains the epitope for the monoclonal antibody PAb240, which is concealed in the wild-type structure but accessible in both mutant structures. In order to confirm this conformational shift, tumor tissue and serum from vinyl chloride-exposed individuals with angiosarcomas of the liver were examined by immunohistochemistry and enzyme-linked immunosorbent assay. Individuals with tumors that contained the p53 mutations were found to have detectable mutant p53 protein in their tumor tissue and serum, whereas individuals with tumors without mutations and normal controls did not.

KEY WORDS: p53; mutation; vinyl chloride; molecular dynamics; immunohistochemistry; angiosarcoma.

1. INTRODUCTION

The most frequently identified site for mutations in human cancers is the p53 tumor suppressor gene (Lane, 1994; Selter and Montenarh, 1994; Soussi *et al.*, 1994). The encoded wild-type p53 protein is known to bind to specific DNA sequences activating the transcription of genes some of which result in cell growth arrest, and this function is thought to be important for the maintenance of the integrity of the genome in response to DNA damage (Lane, 1994; Selter and Montenarh, 1994; Soussi *et al.*, 1994). The majority of cancer-related mutations in p53 cluster in several "hot-spot" regions of the protein that have been highly conserved throughout evolution. These regions

[1] Division of Environmental Health Sciences, Columbia University School of Public Health, New York, New York 10032.
[2] Stine-Haskell Research Center, DuPont Agricultural Chemicals, P.O. Box 30, Newark, Delaware 19714.
[3] Unité de Recherche sur les Hépatites, le Sida et les Retrovirus Humains, INSERM, 69424 Lyon, France.
[4] Oncogene Science, Cambridge, Massachusetts 02142.
[5] Department of Pathology and Laboratory Medicine, Veterans Affairs Medical Center, Brooklyn, New York 11209, and Department of Pathology, SUNY Health Science Center, Brooklyn, New York 11203.
[6] To whom correspondence should be addressed.

0277-8033/96/0500-0367$09.50/0

occur in the sequence-specific DNA-binding core domain of the protein between amino acid residues 102 and 292 (Lane, 1994; Selter and Montenarh, 1994; Soussi *et al.,* 1994). The mutations in p53 found in malignancies could thus result in substitutions of amino acid residues in these regions that are critical for the determination of the structure, and hence cell-cycle inhibitory function, of the protein, contributing to the development of cancer. Another result of this presumed structural change in p53 appears to be a stabilization of the mutant proteins such that they have greatly prolonged half-lives compared with wild-type p53 causing intra- and extracellular accumulations of the mutant proteins in many cases (Lane, 1994; Selter and Montenarh, 1994; Soussi *et al.,* 1994).

Using conformational energy analysis, we have previously examined the local conformational effects of amino acid substitutions (some of which have been associated with specific environmental mutagen exposures) in several of these "hot-spot" regions of p53 (Brandt-Rauf *et al.,* 1992, 1994). We suggested that the observed local conformational effects in these regions may be responsible for the major structural change from a wild-type to a mutant conformation of p53 that has been proposed to occur on the basis of the observed gain or loss of detectability of specific immunologic epitopes between the wild-type and mutant proteins (Brandt-Rauf *et al.,* 1992, 1994). The X-ray crystal structure of a portion of the wild-type p53 protein encompassing the core domain (residues 94 to 312) has now been determined (Cho *et al.,* 1994). Therefore, starting from this structure, we have now used molecular dynamics calculations to compute and compare the average structures of three forms of this core domain of p53: the wild-type protein, the protein with an Arg→Trp substitution at position 249, and the protein with an Ile→Phe substitution at position 255. The latter two substitutions lie in one of the "hot-spot" regions of the core domain and result from A→T transversions at the first base of the respective codons in the p53 gene, as have been found to occur in angiosarcomas of the liver in humans exposed to the carcinogen vinyl chlroide (Hollstein *et al.,* 1994). In order to further correlate our computational findings with changes in the p53 protein *in vivo,* we have also used immunologic techniques to examine the type and level of expression of p53 protein in vinyl chloride-exposed individuals with angiosarcomas of the liver with and without these mutations in the tumor DNA.

2. METHODS

2.1. Molecular Dynamics Analyses of p53 Mutants

The starting structure for the wild-type p53 protein from amino acid residues 94–312 was generated from the X-ray crystal coordinates, including the tetrahedrally coordinated zinc atom (Cho *et al.,* 1994). The entire structure was then subjected to energy minimization using both ECEPP and AMBER potential functions, the latter with a distance-dependent dielectric constant, as described previously (Monaco *et al.,* 1995*a, b*).

The resultant minimized wild-type structure was used as the starting structure for constructing the conformations of the two mutant transforming proteins, Trp 249-p53 and Phe 255-p53. For both mutant proteins, the substituted amino acid was introduced in the energy-minimized wild-type structure in place of the normally occurring amino acid at that position, i.e., Trp for Arg 249 or Phe for Ile 255. The backbone dihedral angles for each substituted residue were the same as for the corresponding amino acid in the wild-type protein. Starting side-chain conformations for each of these residues were the lowest energy conformation ones for the given backbone conformation as determined by ECEPP. These structures were then subjected to nested molecular dynamics and energy minimizations, as described previously (Monaco *et al.,* 1995*a, b*).

The lowest energy structures from this process were then subjected to temperature equilibration at 300°K. Dynamics runs were then performed for a total of 322 psec for the wild-type and 494 and 578 psec for the Trp-249 and Phe-255 mutants, respectively. The total conformational energy converged to a minimum value for each structure, and the last 50 isoenergetic structures on the trajectory of each protein were employed in computing the average structure and the coordinate fluctuations.

Each average structure for the oncogenic forms was superimposed on that for the wild-type protein such that the rms deviation of the coordinates of the backbone atoms of one average structure from the other was a minimum. The average rms

deviation between both of the oncogenic proteins and the wild-type protein was determined for each amino acid residue (Dykes *et al.*, 1993; Liwo *et al.*, 1994; Monaco *et al.*, 1995*a*, *b*).

2.2. Immunologic Analyses of p53 Mutants

Five-micrometer sections of formalin-fixed, paraffin-embedded tumor tissue were obtained from the angiosarcomas of the liver of four individuals heavily exposed to vinyl chloride. DNA from each of these tumors had been previously examined for the presence of mutations in exons 5–8 of the p53 gene, which encompasses the core domain of the protein. One tumor had been found to contain an AGG→TGG mutation at codon 249 (corresponding to an Arg→Trp amino acid substitution) and another an ATC→TTC mutation at codon 255 (corresponding to an Ile→Phe amino acid substitution), whereas the other two tumors did not contain p53 gene mutations (Hollstein *et al.*, 1994). After routine deparaffinization and graded rehydration, tissue sections were stained for the amount of nuclear p53 protein by immunohistochemistry using the primary mouse monoclonal antibody DO-1 and a secondary antibody-horseradish peroxidase system (Vectastain; Vector Labs, Burlingame, Ca), by a previously described method (Luo *et al.*, 1996). A similarly stained A431 human cancer cell line known to contain mutant p53 and LS174T human cancer cell line known not to contain mutant p53 were employed as positive and negative controls, respectively. Each section was analyzed for p53 immunostaining using the CAS 200 computerized imaging system (Cell Analysis Systems, Elmhurst, IL) based on the sum of the optical density of nuclear staining of approximately 10 cells in each of 10 randomly selected fields (i.e., at least 100 cells), and sections were compared based on differences in these optical density distributions. Sections with statistically significant elevated amounts of p53 staining were confirmed as mutant p53 by immunohistochemistry performed the same way but using the primary mouse monoclonal antibody PAb240, which is specific for the epitope between amino acid residues 212 and 217 of the p53 protein, which is not detectable in the wild-type protein (Stephen and Lane, 1992).

In addition, stored frozen serum samples were available from each of these tumor cases as well as from five age-sex-race-matched normal healthy controls. Since we have previously demonstrated that individuals with p53 gene mutations and accumulations of increased amounts of mutant p53 proteins in their tumor tissue often also have detectable mutant p53 protein in their serum (Luo *et al.*, 1994), these serum samples were analyzed for the presence of mutant p53 protein. Analyses were performed using an enzyme-linked immunosorbent assay based on the mutant epitope-specific PAb240 antibody, as described previously (Luo *et al.*, 1995).

3. RESULTS

The final average structure for the wild-type p53 protein was found to differ from the starting X-ray crystal structure by an overall rms deviation of 3.1 Å. The principal contribution to this rms deviation came from a large 11-Å deviation in the segment around amino acid residue 180 in the region designated as loop 2–helix 1 in the X-ray crystal structure (Cho *et al.*, 1994) (results not shown).

Coordinate fluctuations for the wild-type and two mutant p53 proteins are shown in Fig. 1. Coordinate fluctuations for all residues in all proteins are less than 2 Å (and most are less than 1.5 Å), except for amino acid residue 178 in the wild-type protein, for which the fluctuation is approximately 2.1 Å. This fluctuation occurs in the same region where the major difference occurs between the energy-minimized X-ray structure and the average structure for the wild-type protein. These observations suggest that the region around residue 180 may exhibit substantial flexibility. This result is somewhat surprising in view of the fact that residues 178 and 180 flank the zinc-binding residue, His 179, the fluctuation for which is only 1 Å.

Since large differences in structures contributing to the average structure for each protein would be expected to be reflected in relatively large coordinate fluctuations, these low fluctuations for all three proteins suggest that the proteins converge on specific structures that lie close to the average structure in each case. Thus, the average structures can be considered representative of each protein and can be compared to determine structural similarities and differences among them.

The overall rms deviations for the average structures of the Trp-249 and the Phe-255 mutants from the average wild-type structure were 3.5 and 4.0 Å, respectively. The residue rms deviations for

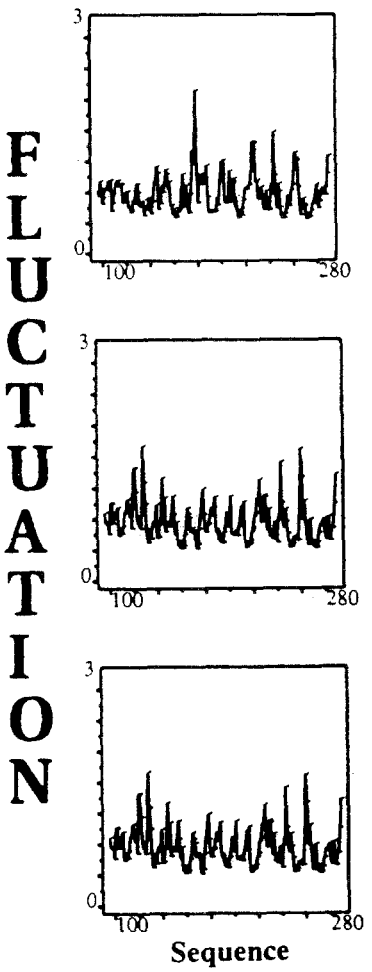

Fig. 1. Fluctuations for the last 50 low-energy structures on the dynamics trajectory of p53 proteins; wild-type protein (upper panel); Trp 249 mutant (middle panel); Phe 255 protein (lower panel). Scales are in angstroms.

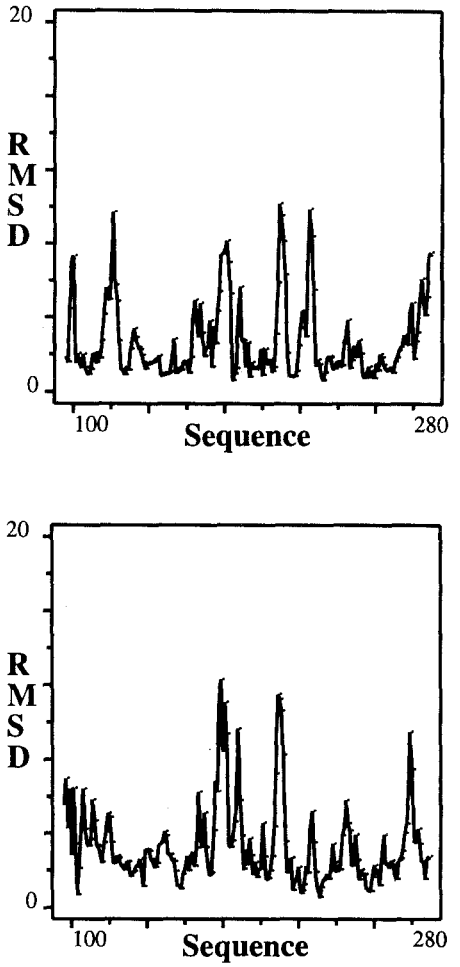

Fig. 2. Individual residue backbone deviations for the coordinates of corresponding amino acid residues of the Trp-249 protein (upper panel) and the Phe-255 protein (lower panel) from those of the wild-type average structure. Scales are in angstroms.

the average structure of each mutant protein compared to the average structure of the wild-type protein are shown in Fig. 2. The rms deviations from the wild type at substituted residues 249 and 255 in each of the respective mutant proteins can be seen to be less than 2 Å. However, for both mutants, there are particular discrete regions that demonstrate wide deviations (greater than 4 Å) from the wild-type protein. Excluding the end-effect deviations at the amino and carboxyl termini, these regions are from amino acid residues 113–124, 172–190, 204–217, 223–228, and 275–281. It should be noted that all of these regions include parts of surface loop domains. Residues 113–124 and 275–281 are included in DNA-binding domains of the p53 protein. The 172–190 region incudes His 179, involved in coordination to zinc. Residues 204–217 contain the epitope recognized by the PAb240 antibody in the mutated forms of p53. Residues 223–228 do not have known function and occur on the opposite side of the protein from the DNA-binding site.

In both mutants, two of these regions exhibit extremely large rms deviations (8–12 Å) from the wild type. These deviations can be seen in Fig. 3, which presents stereo views of the average structure for the Trp-249 and Phe-255 mutants superimposed on the average wild-type structure. In particular, there is a large shift from the wild-type structure in the region 204–217 in each mutant. In the wild-type structure, this region is folded up and under the loop–helix region from residues 166–192 packing into the hydrophobic core of the β-sandwich structure of the protein and thus is not

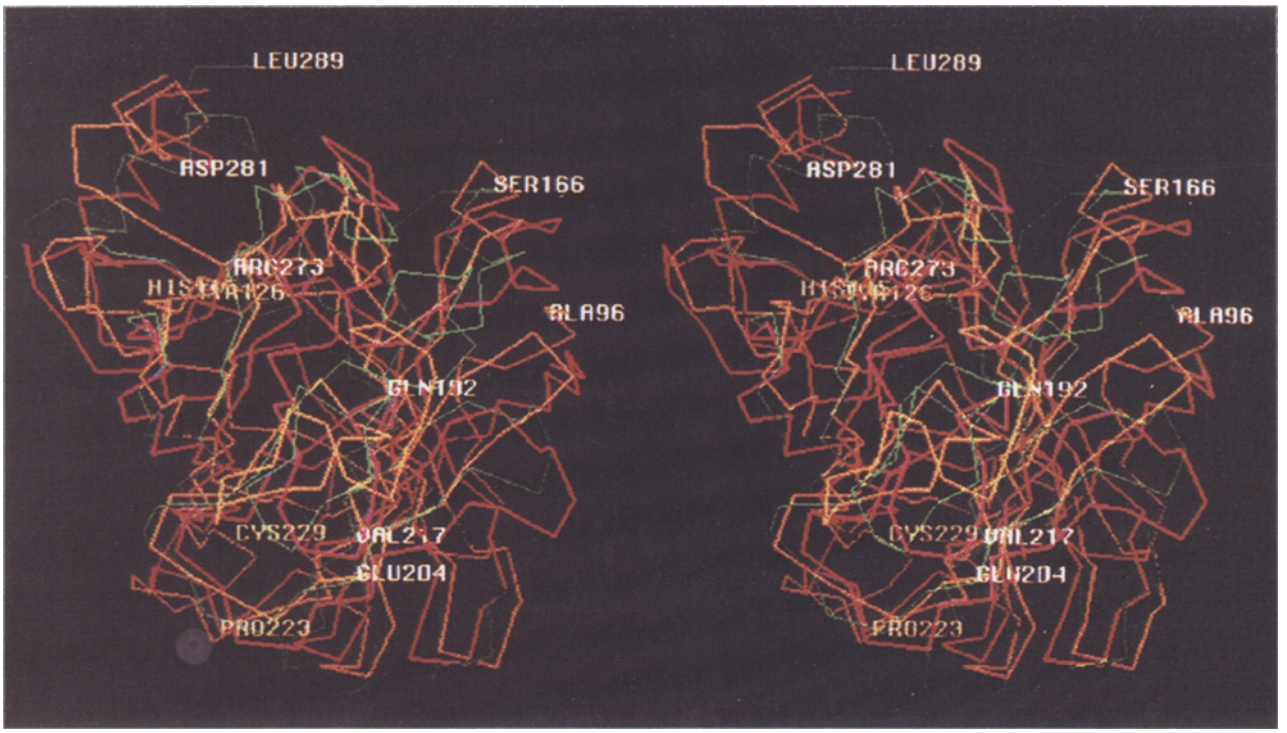

Fig. 3. Stereo view of the superimposed Cα traces of the average structures of the wild-type (orange), Trp-249 (green), and Phe-255 (purple) p53 proteins obtained from molecular dynamics simulations. The numbered residues have been placed on the wild-type average structure. Note the region from residues 204–217, which is clearly exposed in the mutant proteins on the right-hand side of the figure.

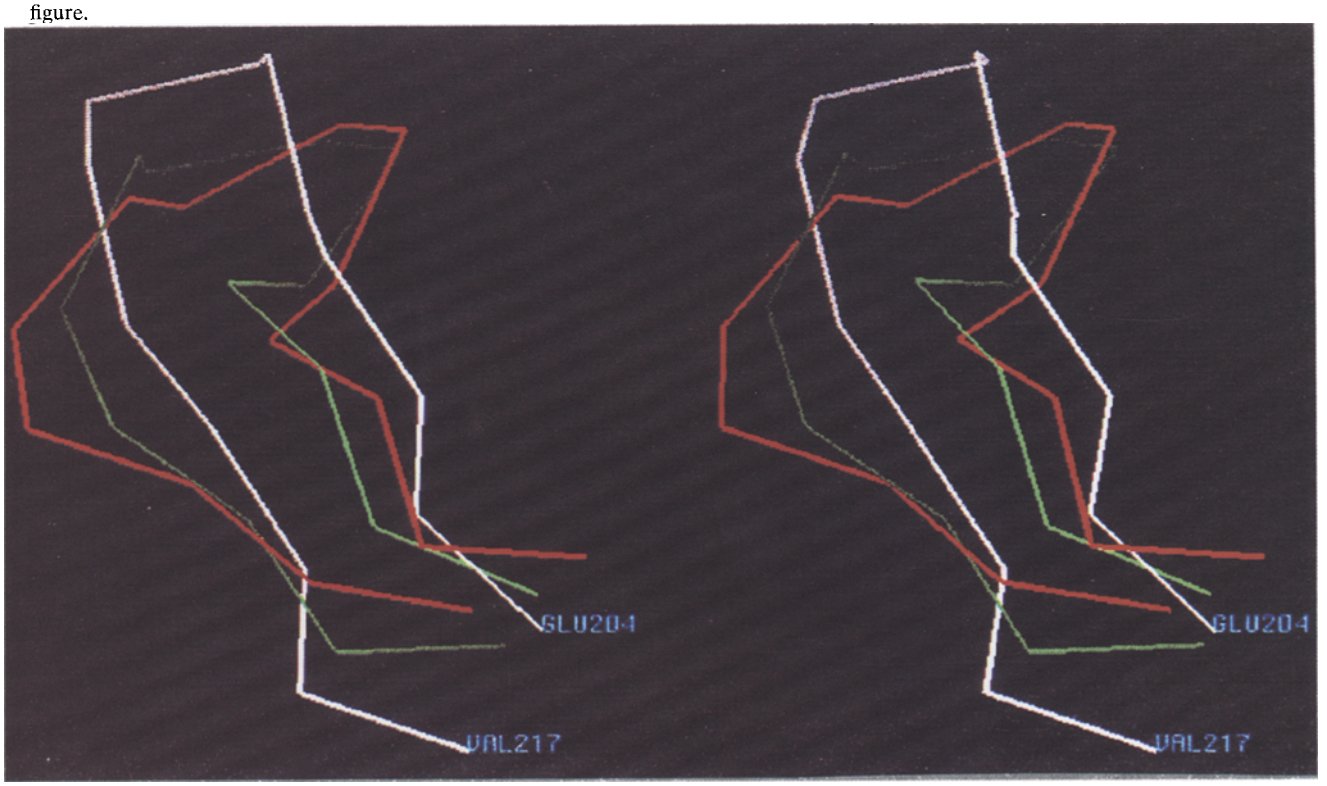

Fig. 4. Stereo view of the superimposed Cα traces of the average structures of the region from residues 204–217 in the wild-type (gray) and Trp-249 (green) and Phe-255 (red) mutant p53 proteins.

exposed. In both mutants, this region is bent down and away from the 166–192 loop–helix region and the β-sandwich core and is exposed. As noted, this region contains the epitope for the monoclonal antibody PAb 240, which is thus clearly exposed in each of the mutant proteins.

Although the average structures for the two mutant proteins can be seen to be distinctly different from the average wild-type structure and to share certain regions of deviation in common, it should be noted that the two mutant structures are not identical and in fact have an overall rms deviations between them of 3.9 Å. However, this overall deviation obscures other important similarities. For example, if the 204–217 region alone is compared among the three proteins, the two mutant structures are seen to be closely superimposable on one another, but not on the corresponding wild-type structure (Fig. 4). Thus, while the structures of this epitope region are displaced from one another in the two mutant proteins, their individual conformations are quite similar to one another. Since the epitope region in both mutants is also much more exposed on the surface than is the corresponding region of the wild-type protein, selective binding of PAb240 to both mutant forms can be understood. The epitope region of both mutants is exposed and has the same conformation, enabling antibody recognition to occur.

Since both mutant proteins apparently undergo significant regional changes in structure compared with the wild-type protein, these altered domains may be detectable immunologically, such as the 204–217 region containing the PAb240 epitope. Detection of these altered proteins provides confirmation of the predicted structural shifts and may be useful in early tumor detection. To this end, as noted, we studied the tissue and sera of patients with known exposure to vinyl chloride who developed angiosarcomas of the liver.

As can be seen in Table I, immunohistochemical analysis of the angiosarcomas of the liver confirmed that the tumors with Trp-249 and Phe-255 mutations contained increased amounts of mutant p53 protein. Typical results are shown in Figs. 5 and 6 demonstrating the statistically significant increases in mutant p53 found in the tumors with mutations compared to normal liver tissue ($p < 0.001$). In addition, the serum samples from the individuals with tumors with p53 mutations had elevated amounts (greater than five times the limit of detection of the assay, i.e., greater than 0.25 ng/ml) of mutant p53 protein based on the assay with PAb240, whereas the serum samples from individuals with tumors without mutations and from five normal controls were negative for mutant p53 (see Table I). Thus, each substitution in p53 results in the immunological detection of an epitope not present in the normal protein due to the structural shifts in the 204–217 region induced by the two substitutions.

4. DISCUSSION

These results suggest that specific amino acid substitutions in the core domain of the p53 protein that are related to specific carcinogen-induced mutations in the p53 gene that occur in associated sentinel neoplasms are likely to produce distinct conformational changes in the protein. Although the local conformational changes in the protein at the site of the amino acid substitutions are

Table I. Results of Analyses for Mutant p53 in Vinyl Chloride-Exposed Workers and Unexposed Controls

	Presence of p53 gene mutation	Immunohistochemistry for mutant p53 protein	Serum ELISA for mutant p53 protein
ASL cases[a]			
1	+	+	+
2	+	+	+
3	–	–	–
4	–	–	–
Total	2/4+	2/4+	2/4+
Controls			
Total		0/5+	0/5+

[a] ASL, angiosarcoma of the liver.

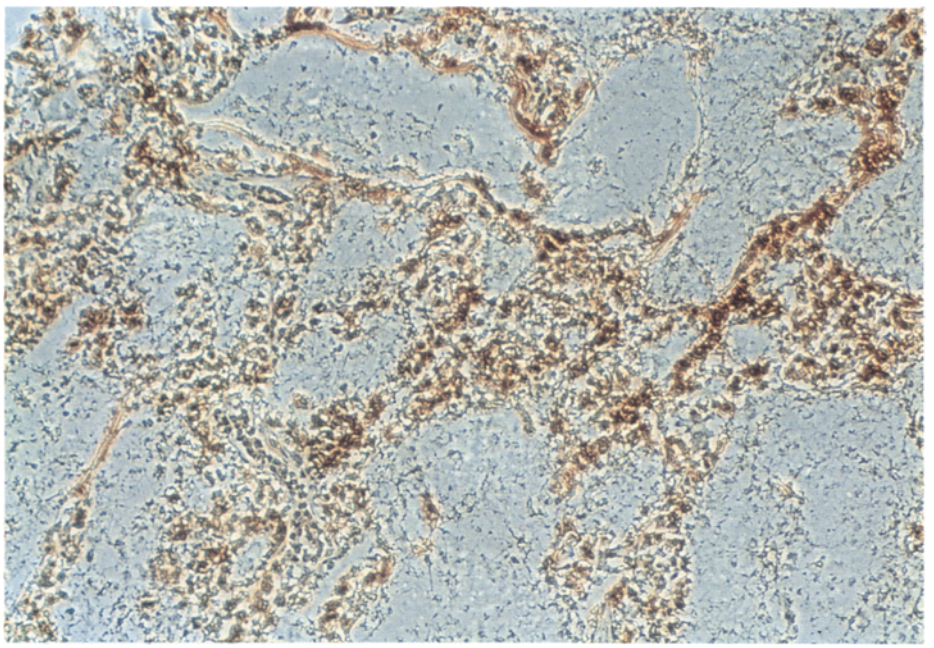

Fig. 5. Representative immunohistochemistry for mutant p53 protein of angiosarcoma of the liver known to contain a p53 mutation with immunoperoxidase staining (100×); reduced 25% for reproduction.

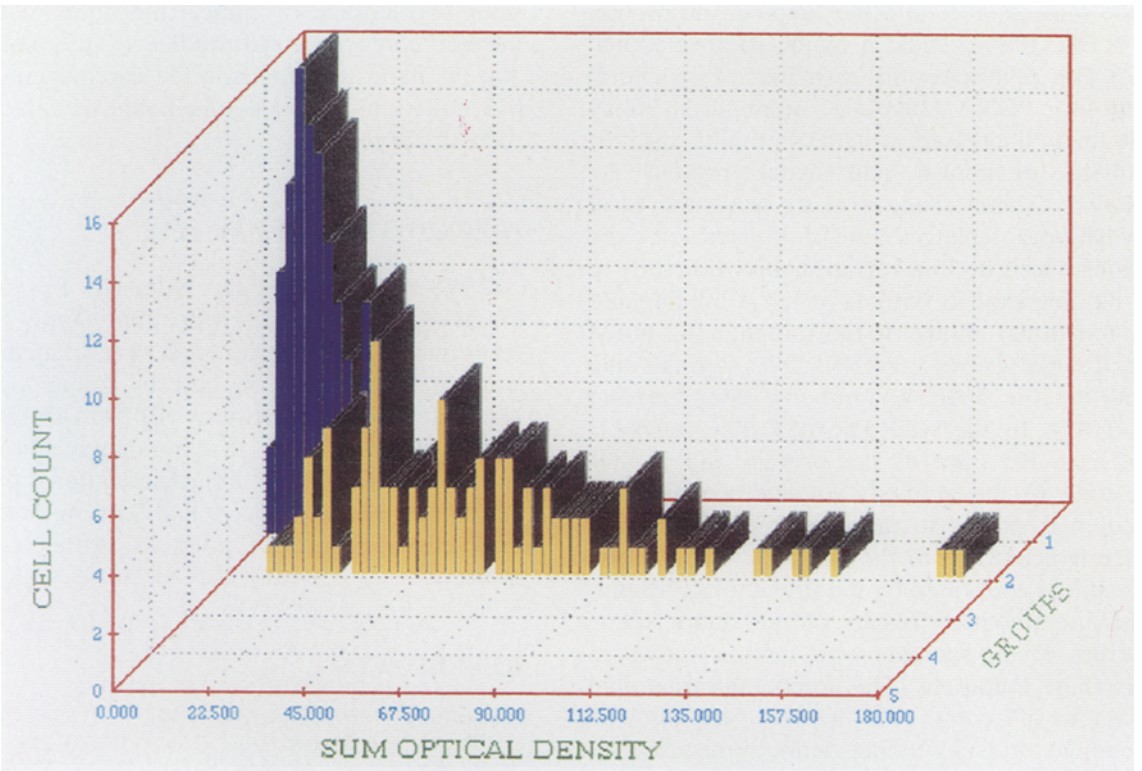

Fig. 6. Representative densitometric analysis of the sum of the optical densities of intranuclear immunohistochemical mutant p53 staining of normal liver (group 1) and an angiosarcoma of the liver known to contain a p53 mutation (group 2) from formalin-fixed, paraffin-embedded tissue sections. Approximately ten cells in ten randomly selected fields were analyzed for each group. The difference in the optical density distributions is statistically significant ($p < 0.001$).

relatively small, they apparently induce large long-range conformational shifts in other regions of the protein, as we had suggested previously (Brandt-Rauf *et al.,* 1992, 1994).

On the basis of the X-ray crystal structure of the core domain of the wild-type p53, it has been suggested that such amino acid substitutions would be more likely to result in globally denatured states of p53 rather than a well-defined, alternative "mutant conformation" for the protein (Cho *et al.,* 1994). However, the results of this study demonstrating specific, discrete conformational changes in p53 that appear in common regions for two different p53 mutants strongly suggest that the mutant proteins are not totally denatured, but rather adopt relatively distinct "mutant conformations."

The common features of these conformations include major shifts in the regions from amino acid residues 172–190 and 204–217. Residues in the former region (172–190), including Arg 175, play a critical role in stabilizing the structure of the DNA-binding surface of p53 through hydrogen bonding with residues in other loops of the protein (Cho *et al.,* 1994). Thus, a major conformational shift in this region results in a loss of structural stability for DNA binding, although it may contribute to increased structural stability against proteolytic breakdown and hence protein accumulation. These changes along with the local conformational changes at the sites of the mutations which lie in a region involved directly in DNA binding explain the loss of DNA binding and hence functional ability of the mutants. As noted above, the latter region (204–217) contains the epitope for the PAb240 antibody (Stephen and Lane, 1992). In the wild-type p53, this region is packed into the core of the protein and is thus inaccessible to the antibody. In the two mutants, this region is shifted to the surface of the protein and clearly accessible to the antibody. The validity of this shift is confirmed by the immunohistochemical and immunoassay results of the tumor tissue and serum of the patients with tumors known to contain these mutations. The noted conformational changes in p53 may also help to explain the development of a circulating antibody response to p53 in one of the cases of ASL with a p53 mutation (Trivers *et al.,* 1995), based on the notion that the body's immune system recognizes the conformationally altered protein as foreign. Similar antibody responses have been noted in a number of patients with different cancers that contain other p53 mutations (Soussi *et al.,* 1994). Analysis of such other amino acid substitutions in p53 will be necessary to confirm that the regions of conformational shifts noted here are common for a wide range of transforming p53 mutations.

The immunologic analyses also indicate that in certain cases the PAb240 epitope shift may be reliably used as a biomarker to detect the p53 conformational change both intracellularly and in the extracellular environment. Thus, it is interesting to note that serum mutant p53 has also been detected by the presence of the PAb240 epitope using the same ELISA in 3 of 19 individuals who have been heavily exposed to vinyl chloride but who do not yet have detectable neoplastic lesions, and that degree of vinyl chloride exposure correlated with increased likelihood of the presence of the mutant p53 (Smith *et al.,* 1996). Such a serologic biomarker may therefore be of value in identifying individuals who have sustained a cancer-related p53 mutation and are thus presumably at risk for the development of cancer prior to the time of clinical detection of disease. Further conformational studies of p53 should be able to indicate which specific carcinogen-induced p53 mutations would be amenable to detection by such an approach.

ACKNOWLEDGMENTS

We wish to thank Dr. Nikola P. Pavletich for kindly providing us with the X-ray crystal coordinates of the wild-type core domain. This work was supported in part by grants from the National Cancer Institute (R01-CA42500, R01-CA69243), the U.S. Environmental Protection Agency (R818624), the Association pour la Recherche sur le Cancer, and le Groupment des Enterprises Françaises pour la Lutte contre le Cancer.

REFERENCES

Brandt-Rauf, P. W., DeVivo, I., Dykes, D. C., and Pincus, M. R. (1992). *J. Biomol. Struct. Dynam.* **10,** 253–264.

Brandt-Rauf, P. W., Monaco, R., and Pincus, M. R. (1994). *Proc. Natl. Acad. Sci. USA* **91,** 9262–9266.

Cho, Y., Gorina, S., Jeffrey, P. D., and Pavletich, N. P. (1994). *Science* **265,** 346–355.

Dykes, D. C., Friedman, F. K., Luster, S. M., Murphy, R. B., Brandt-Rauf, P. W., and Pincus, M. R. (1993). *J. Biomol. Struct. Dynam.* **11,** 443–458.

Hollstein, M., Marion, M.-J., Lehman, T., Welsh, J., Harris, C. C., Martel-Planche, G., Kusters, I., and Montesano, R. (1994). *Carcinogenesis* **15,** 1–3.

Lane, D. P. (1994). *Br. Med. J.* **50,** 582–599.

Liwo, A., Gibson, K. D., Scheraga, H. A., Brandt-Rauf, P. W., Monaco, R., and Pincus, M. R. (1994). *J. Protein Chem.* **13,** 237–251.

Luo, J.-C. Zehab, R., Anttila, S., Ridanpaa, M., Husgafvel-Pursiainen, K., Vainio, H., Carney, W., DeVivo, I., Milling, C., and Brandt-Rauf, P. W. (1994). *J. Occup. Med.* **36,** 155–160.

Luo, J.-C., Neugut, A. I., Garbowski, G., Forde, K. A., Treat, M., Smith, S., Carney, W. P., and Brandt-Rauf, P. W. (1995). *Cancer Lett.* **91,** 235–240.

Luo, J.-C., Neugut, A. I., Garbowski, G., Forde, K. A., Treat, M., Smith, S., Niman, H., and Brandt-Rauf, P. W. (1996). *Biomarkers,* **1,** 29–33.

Monaco, R., Chen, J. M., Chung, D., Brandt-Rauf, P. W., and Pincus, M. R. (1995*a*). *J. Protein Chem.* **14,** 457–466.

Monaco, R., Chen, J. M., Friedman, F. K., Brandt-Rauf, P. W., Chung, D., and Pincus, M. R. (1995*b*). *J. Protein Chem.* **14,** 721–730.

Selter, H., and Montenarh, M. (1994). *Int. J. Biochem.* **26,** 145–154.

Smith, S., Marion, M.-J., Luo, J.-C., and Brandt-Rauf, P. W. (1996). *Occup. Environ. Med.,* in press.

Soussi, T., Legros, Y., Lubin, R., Ory, K., and Schlichtholz, B. (1994). *Int. J. Cancer* **57,** 1–9.

Stephen, C. W., and Lane, D. P. (1992). *J. Mol. Biol.* **225,** 577–583.

Trivers, G. E., Cawley, H. L., DeBenedetti, V. M. G., Hollstein, M., Marion, M.-J., Bennett, W. P., Hoover, M. L., Prives, C. C., Tamburro, C. C., and Harris, C. C. (1995). *J. Natl. Cancer Inst.* **87,** 1400–1407.